Optimization of the METIS on-board algorithm for the automatic detection of Coronal Mass Ejections

A. Bemporad[1] & G. Guilluy[1,2]

[1]INAF-Turin Astrophysical Observatory, Italy
[2]Physics Department, University of Turin, Italy

Abstract

The Solar Orbiter-METIS on-board algorithm for the automated detection of Coronal Mass Ejections and the release of a "CME flag" has been tested and optimized based on the analysis of data acquired by the STEREO-COR1 and COR2 coronagraphs. The polarized images by STEREO acquired with 3 different orientations of the linear polarizer have been combined and analysed to reconstruct the polarized sequences that will be acquired by METIS with 4 different polarization angles. The images have been then divided into 8 angular sectors, to simulate the lightcurves and normalized running differences that will be measured by METIS. For the derivation of lightcurves, different circular crown areas with different radial extensions have been considered, in order to define the optimal interval. Results show that the on-board algorithms will be able to successfully identify the occurrence of CMEs at both heliocentric distances of 0.28 AU and 0.72 AU. Among possible different areas, for optimal operations of this algorithm it is suggested to employ circular crown areas centred over the inner fraction of the instrument field of view, and possibly with smaller radial extensions. The work described here was performed in 2015 for a triennial Degree Thesis in Physics at Turin University Physics Department.

1. Introduction

METIS (Antonucci et al. 2020) is the multi-channel coronagraph for the ESA-Solar Orbiter mission, successfully launched in February 2020. The instrument is now providing the first ever observations of the solar corona at the same time in two different channels corresponding to two different wavelength intervals:

- VL (visible light) channel (broadband between 580 – 640nm)
- UV channel (narrow band with a 10 Å bandpass centered at 121.5nm for HI Lyman-α line)

The visible channel includes a Polarimeter that will provide the means to detect and to observe the linearly polarized component of the K corona. METIS exploits for the first time the innovative design of an inverted occulter coronagraph, i.e. a circular aperture on the Solar Orbiter thermal shield that will act as coronagraph entrance pupil (Fineschi et al. 2020).

As for the other 5 remote sensing instruments on-board Solar Orbiter, due to limitations in the available telemetry for data download, for each orbit of the spacecraft (about 6 months) the observations will be concentrated over 3 time intervals, each one with a duration by 10 days: 1 interval centred on the time of perihelion passage, and two more intervals centred on the time of maximum (in absolute value) heliolatitude. During the first orbits the perihelion will occur at an heliocentric distance of about 0.28 AU, while the high-latitude observations will be performed with the spacecraft at a distance of about 0.72 AU, even if these

values are changing during the mission and depend on the considered orbit (Bemporad 2009). During observation any communication with the satellite will be, when possible, very limited, and the remote sensing instruments will have to proceed with their observations independently.

In particular, in the occasion of major Coronal Mass Ejections (CMEs) the METIS Coronagraph on-board Solar Orbiter spacecraft will be able to provide in output a "CME flag" to be issued to the other remote sensing instruments (Bemporad et al. 2014). The aim of the flag will be 1) to automatically start the "CME observation program", 2) to provide an internal alert for the occurrence of a major CME to other on-board instruments, 3) to identify the main CME latitude of propagation, and 4) to disentangle between the occurrence of halo and non-halo CMEs. The aim of this work has been:

- to characterize the VL intensity variations (hence the algorithm threshold) that will be observed by METIS coronagraph during different phases of the orbit of Solar Orbiter, and
- to understand how the algorithm for the automatic detection of CMEs could be optimized using different areas for the computation of the intensity averaged over different angular sectors.

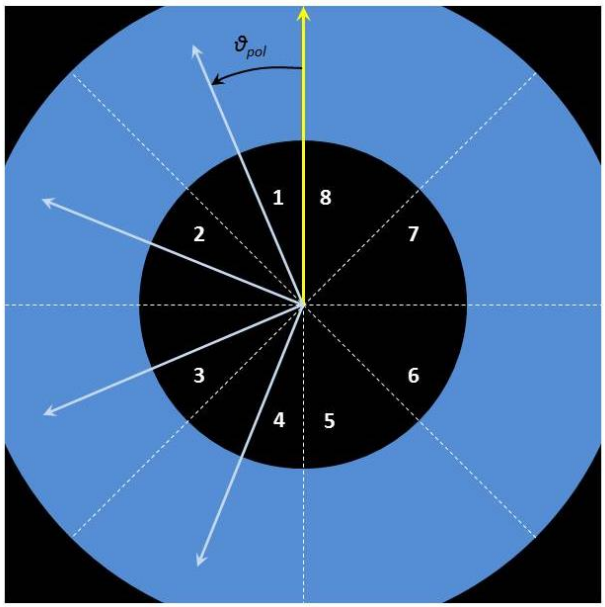

Figure 1: the METIS field of view and the location of 8 angular sectors for the estimate of the CME flag delimited by white dashed lines. The Figure also shows the 4 orientations of the linear polarizer for a typical METIS polarized sequence.

2. Analysis general description

Given the limits in the CPU computational capabilities (the METIS CPU will be able to work at 10 MFlops, to be compared with typical ~50-150 GFlops of commercial PCs and ~10-30 GFlops of common smartphones), the algorithm have to be based on very simple and computationally fast logical operations (Pancrazzi et al. 2014). For this reason, each image will be divided in 8 angular sectors and the algorithm will work on a simple array of 8 elements corresponding to the total VL intensity observed over the 8 angular sectors. In order to simplify as more as possible the computation of the 8 elements, the 8 angular sectors will be oriented in order to have their edges parallel to the detector columns and rows, as it is shown in Figure 1.

Given the above locations for 8 angular sectors, in what follows we assume that each METIS polarized sequence will consist typically of 4 polarized images acquired with 4 different orientations ϑ_{pol} of the linear polarizer. In particular, we assume that in each exposure the linear polarizer will be oriented at angles

corresponding to the bisector of each angular sector, hence at angles of 22.5°, 67.5°, 112.5° and 157.5° (measured counter-clockwise as it is shown in Figure 1).

The flag optimization analysis has been performed with these subsequent steps:

- Selection of 10 eruptive events (limb and partial halo CMEs) observed by STEREO coronagraphs;
- Download of polarized sequences (triplets) acquired by both COR1 and COR2 telescopes;
- Construction of corresponding METIS polarized sequences (quadruplets);
- Extraction of the lightcurve vectors time evolution with different circular crowns;
- Analysis of the time evolution resulting with different circular crowns.

All the above steps are described in details in the next Sections.

In this analysis we analysed both COR1 and COR2 images in order to determine if and how the algorithm will depend on different observational periods during the spacecraft orbit, hence on the heliocentric distance of observation. In fact, the METIS field of view (FOV) will go from 1.5° up to 3.0° and this will correspond to different projected altitudes in the corona depending on the considered heliocentric distance of the spacecraft. In particular:

- at perihelion (0.28 AU): FOV from 1.58 to 3.15 solar radii,
- at high latitude (0.72 AU): FOV from 4.06 to 8.12 solar radii.

If the above interval are compared with the FOV extension of the COR1 (1.1 – 3.0 solar radii) and COR2 (2.0 – 15 solar radii) it turns out that a good approximation for the expected evolution of CMEs observed by METIS is provided by COR1 and COR2 images respectively for the perihelion and the high latitude observation intervals.

3. Selection of the eruptive events

The events have been selected by visual inspection of the SECCHI/COR2 catalogue available on-line[1] and based on the SEEDS (Solar Eruptive events Detection System) algorithm (Olmedo et al. 2008). In particular the selected 10 events are listed in Table 1. Notice that "Start times" provided in this Table correspond to the time of the first frame where the CME has been identified at first from the SEEDS algorithm, and not to the real CME start time.

n.	Day (DD/MM/YYYY)	Start time	Central PA	Angular width	Linear fit
1	04/06/2011	22:24:00	310°	134°	1800 km/s
2	24/03/2012	01:24:41	399°	210°	1062 km/s
3	23/07/2012	03:54:28	449°	235°	1217 km/s
4	05/03/2013	04:54:00	288°	204°	1139 km/s
5	11/04/2013	07:54:00	93°	186°	696 km/s
6	28/08/2013	16:24:30	172°	160°	735 km/s
7	29/09/2013	22:54:42	331°	99°	642 km/s
8	25/02/2014	01:24:55	249°	104°	1502 km/s
9	10/06/2014	14:24:00	242°	210°	113 km/s
10	22/09/2014	08:24:31	416°	128°	556 km/s

Table 1: list of the events selected for the METIS flag test described here.

[1] http://spaceweather.gmu.edu/seeds/secchi.php

These events have been selected among others existing in the catalogue in order to have 10 no slow (v > 600 km/s) limb or partial halo (angular width < 360°) CMEs. One example of one of these events as reported by the SEEDS catalogue is shown in Figure 2. For each event we downloaded from the usual SECCHI online database[2] a total of 20 COR1 triplets and 10 COR2 triplets during the event. Hence a total of 600 COR1 images and 300 COR2 images has been downloaded, corresponding to about 2.7 GB of data. Each triplet consists of 3 polarized images acquired with 3 different orientations of the linear polarizer corresponding to angles of 0°, 120° and 240°. COR1 triplets are acquired at a rate of 1 triplet every 5 minutes, with time differences within different polarizer orientations by 9 seconds or 12 seconds, depending on the observation program. COR2 triplets are acquired at a rate of 1 triplet every hour, with time difference within different polarizer orientations by 30 seconds.

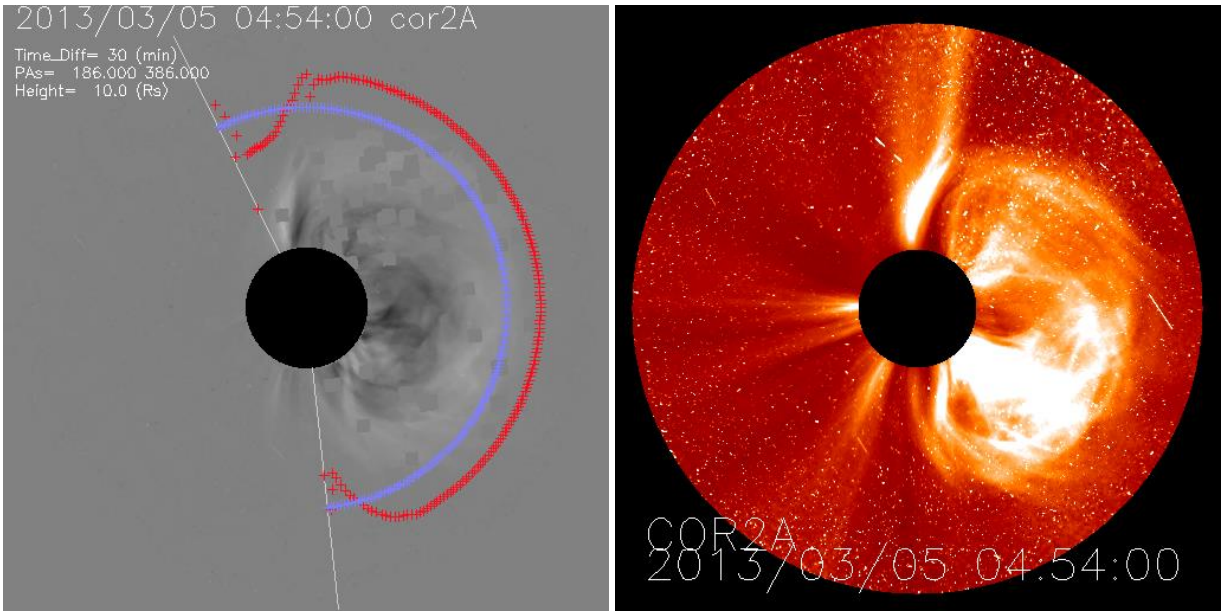

Figure 2: example of one of the selected events as reported by the SEEDS catalogue with regular (right) and running difference (left) COR2A frames.

4. Construction of the METIS polarized sequences

As mentioned, the general METIS polarized sequence will consist of 4 images acquired with 4 different orientations ϑ_{pol} of the linear polarizer. In theory the determination of the 3 elements (I, Q, U) of the Stokes vector (for linear polarization, neglecting circular polarization V which is zero for the K corona) requires only the acquisition of 3 images (m_0, m_1, m_2) with 3 different orientations (ϑ_{pol0}, ϑ_{pol1}, ϑ_{pol2}) of the polarizer. The Stokes vector is then given by

$$\begin{pmatrix} m_0 \\ m_1 \\ m_2 \end{pmatrix} = \begin{pmatrix} 1 & \cos\delta_0 & \sin\delta_0 \\ 1 & \cos\delta_1 & \sin\delta_1 \\ 1 & \cos\delta_2 & \sin\delta_2 \end{pmatrix} \begin{pmatrix} I \\ Q \\ U \end{pmatrix}$$

For the specific case of polarization angles ϑ_{pol0} = 0°, ϑ_{pol1} = 120°, ϑ_{pol2} = 240° (with $\delta_i = 2\,\vartheta_{pol\,i}$) it turns out that the Stokes vector components are given by

[2] http://secchi.nrl.navy.mil/cgi-bin/swdbi/secchi_flight/images/form

$$I = \frac{2}{3}\left(m_0 + m_1 + m_2\right)$$

$$Q = \frac{2}{3}\left(2m_0 - m_1 - m_2\right)$$

$$U = \frac{2}{\sqrt{3}}\left(m_2 - m_1\right)$$

Nevertheless, as demonstrated by previous experience with SOHO and STEREO coronagraphs, the acquisition of a fourth image is mandatory in order to reduce as more as possible the uncertainties in the measured polarization vector. Existing space based coronagraph acquire polarized image sequences only with 3 different orientations of the linear polarizer (usually ϑ_{pol} = 0°, 120° and 240°), hence no quadruplet sequences are available for a test on METIS data. For this reason, in the first part of this work each COR1 and COR2 triplet has been calibrated and the images for the 3 components of the Stokes vector (I, Q, U) have been determined. Calibration and determination of the Stokes vector components has been performed with standard routines provided within *SolarSoftware*. Then, the (I, Q, U) images have been used to create a synthetic quadruplet of COR1 and COR2 images m_i ($_i$ = 0, 1, 2, 3) by assuming 4 different orientations $\vartheta_{pol\,i}$ of the linear polarizer. In particular, the METIS quadruplets have been reconstructed by assuming (ϑ_{pol0} = 22.5°, ϑ_{pol1} = 67.5°, ϑ_{pol2} = 112.5°, ϑ_{pol3} = 157.5°). The generic m_i image is then given by

$$m_i = I + Q\cos\left(2\vartheta_{pol\,i}\right) + U\sin\left(2\vartheta_{pol\,i}\right).$$

In this way, starting from the input 600 COR1 and 300 COR2 images, a total of 800 COR1 and 400 COR2 images with 4 different orientations of the linear polarizer have been created.

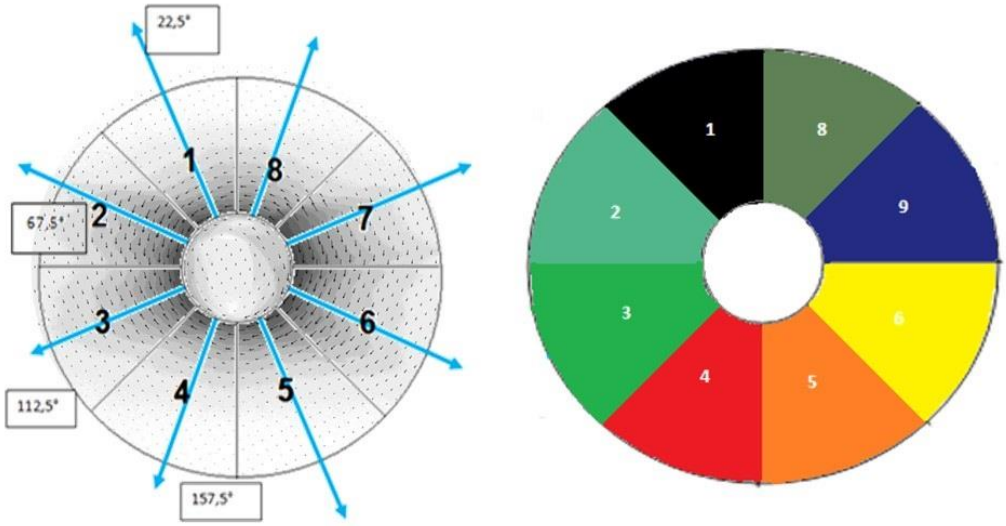

Figure 3, left: the definition of different angular sectors with respect to the coronal polarized emission. Right: color code definition for different angular sectors that is employed in the following Figures.

5. Construction of the METIS lightcurves

The sequences of the METIS polarized images reconstructed from the COR1 and COR2 images have been then analysed to simulate the signal that will be employed by the on-board algorithm. In the VL, the polarized emission from the solar corona is linearly polarized, with the polarization vector always tangent to the solar limb direction, as it is shown in Figure 3. On the other hand, the orientation of the directions of maximum transmission of the linear polarizing filter on-board METIS has been fixed at four different angles to acquire

each polarized sequence, separated each other by a relative rotation angle of 45° around the geometrical centre of the image (corresponding to the optical axis), as mentioned above. Hence, as explained more in details in Bemporad et al. (2014), the on-board algorithm has been designed to extract the 8 lightcurves maximizing the VL emission. In particular, each lightcurve in each one of the 4 images with different orientations of the linear polarizer is extracted by selecting the couple of angular sectors centred on the direction perpendicular to the direction of the linear polarizer. This allows the maximization not only of coronal VL emission, but also of the transient emission associated with CMEs.

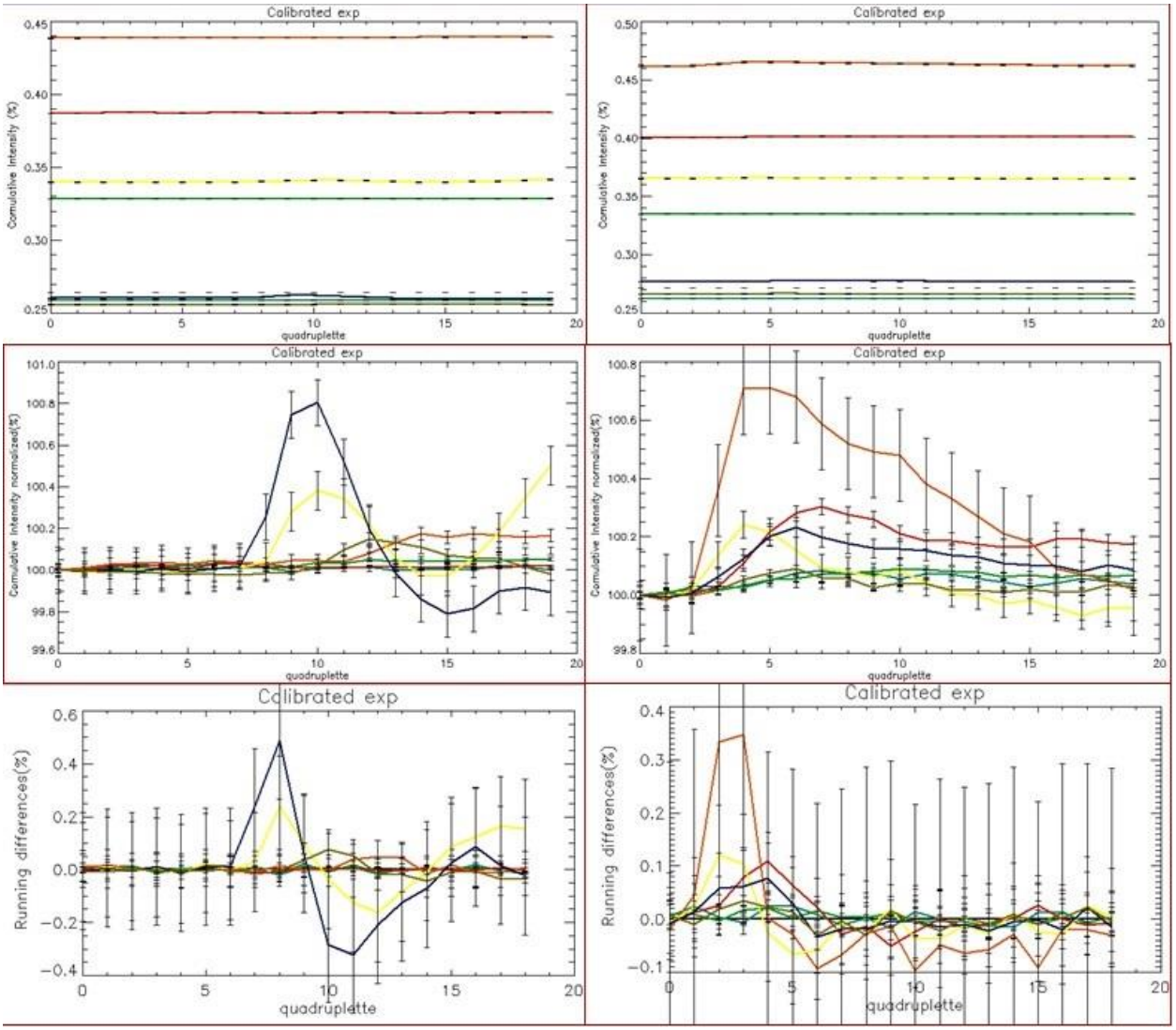

Figure 4, top row: evolution of the absolute total intensity (in arbitrary units) in the 8 angular sectors, with color codes defined in the right panel of Figure 3, for the event of 23 March 2012 (left) and 23 July 2012 (right). Middle row: same as top row, with intensities normalized with respect to the pre-CME intensity. Bottom row: same as top and middle rows, showing the evolution of the running differences.

6. Analysis of the METIS lightcurves

The resulting lightcurves from the 8 angular sectors have been analysed during the occurrence of the selected 10 CMEs (Table 1). In particular, the first plots given in Figure 4 (top row) shows that the absolute intensity values are very different in the 8 angular sectors, and the relative intensity variations during the CMEs are very small. Hence, a single threshold value cannot be identified, and these values cannot be employed to identify automatically on-board the occurrence of CMEs. The CMEs become much more evident once the

intensity values are normalized with respect to the intensity values measured in each sector just before the occurrence of the event (Figure 4, middle row), even if – probably because of the averaging over full angular sectors with angular width by 45° - the measured variations are by less than 1%. Nevertheless, this approach cannot be applied on-board, because it requires to know in principle an average value of the coronal intensity before the CME, but this will change significantly along the spacecraft orbit and depending on the intrinsic evolution of the solar corona. Hence, as explained by Bemporad et al. (2014), it is necessary to consider the evolution of the relative running differences, which means to estimate for each angular sector *i* the relative variation of intensity *I* at time t_j as $\Delta I_{ij} = (I_{ij} - I_{i(j-1)})/I_{ij}$. The values for these quantities are shown in Figure 4 (bottom row) for 2 among 10 of the analysed CMEs; it is clear from these curves that by setting a common threshold for all angular sectors it is possible to identify not only the occurrence of the event, but also the number of angular sectors where the CME is observed, thus allowing to consider in principle two different values of the threshold for limb CMEs or halo CMEs.

Measured intensity variations for different projected altitude intervals of the circular crown areas

	Average altitude (Rsun)	04/06/2011	23/03/2012	23/07/2012	05/03/2013	11/04/2013	28/08/2013	29/09/2013	10/06/2014	25/02/2014	22/09/2014	
comulative intensity differences (%)	2,32	0,8 ± 0,6	0,5 ± 0,2	0,30 ± 0,30	0,58 ± 0,19	1,5 ± 0,9	0,4 ± 0,3	5,4 ± 2,0	0,5 ± 0,3	0,7 ± 0,2	0,7 ± 0,6	COR1
	3,62	0,22 ± 0,12	0,2 ± 0,2	0,17 ± 0,14	0,60 ± 0,19	0,7 ± 0,6	0,05 ± 0,09	0,3 ± 0,3	0,3 ± 0,3	0,6 ± 0,3	0,8 ± 0,8	
	2,97	0,4 ± 0,2	0,4 ± 0,4	0,24 ± 0,17	0,60 ± 0,19	1,3 ± 0,9	0,037 ± 0,010	0,9 ± 0,7	0,4 ± 0,3	0,4 ± 0,3	0,9 ± 0,2	

	Average altitude (Rsun)	04/06/2011	23/03/2012	23/07/2012	05/03/2013	11/04/2013	28/08/2013	29/09/2013	25/02/2014	10/06/2014	22/09/2014	
comulative intensity differences (%)	6,6	4 ± 2	9 ± 2	8 ± 5	11 ± 6	3,5 ± 1,2	8 ± 3	12 ± 3	8 ± 6	7 ± 3	7,5 ± 1,8	COR2
	9	4,6 ± 1,3	6 ± 2	10 ± 3	7 ± 3	6,0 ± 1,5	5 ± 3	5 ± 2	7 ± 5	6 ± 2	6 ± 3	
	11,6	4,0 ± 1,3	3,5 ± 1,8	5 ± 3	6,7 ± 1,7	3 ± 2	3 ± 2	4 ± 2	6 ± 4	5 ± 1,5	4 ± 2	

Measured intensity variations for different radial extensions of the circular crown areas

	d_i [Rsun]	04/06/2011	23/03/2012	23/07/2012	05/03/2013	11/04/2013	28/08/2013	29/09/2013	25/02/2014	10/06/2014	22/09/2014	
comulative intensity differences (%)	0,3	0,4 ± 0,2	0,3 ± 0,3	0,33 ± 0,19	0,9 ± 0,2	2,0 ± 0,7	1,0 ± 0,2	1,1 ± 0,4	0,689 ± 0,300	0,6 ± 0,3	0,23 ± 0,11	COR1
	0,5	0,4 ± 0,2	0,3 ± 0,2	0,34 ± 0,19	0,9 ± 0,2	1,5 ± 0,7	0,7 ± 0,2	0,7 ± 0,4	0,679 ± 0,300	0,5 ± 0,4	0,22 ± 0,11	
	0,8	0,4 ± 0,2	0,3 ± 0,2	0,34 ± 0,20	0,8 ± 0,2	1,1 ± 0,7	0,5 ± 0,2	0,8 ± 0,5	0,643 ± 0,300	0,5 ± 0,3	0,21 ± 0,11	
	1,0	0,4 ± 0,2	0,3 ± 0,2	0,30 ± 0,18	0,7 ± 0,3	1,1 ± 0,7	0,4 ± 0,2	0,5 ± 0,5	0,555 ± 0,300	0,5 ± 0,3	0,160 ± 0,110	
	1,3	0,4 ± 0,2	0,4 ± 0,2	0,24 ± 0,18	0,51 ± 0,19	1,3 ± 0,9	0,4 ± 0,2	0,9 ± 0,6	0,443 ± 0,300	0,4 ± 0,3	0,090 ± 0,110	

	d_i [Rsun]	04/06/2011	23/03/2012	23/07/2012	05/03/2013	11/04/2013	28/08/2013	29/09/2013	25/02/2014	10/06/2014	22/09/2014	
comulative intensity differences (%)	1,1	6 ± 4	7 ± 2	10 ± 4	7 ± 3	5,7 ± 1,2	3,4 ± 1,9	1,0 ± 0,6	5,4 ± 1,2	3,0 ± 1,0	5,2 ± 1,9	COR2
	2,2	3 ± 2	6,5 ± 1,8	6 ± 3	5 ± 3	5,7 ± 1,2	3 ± 2	1,1 ± 0,3	4,8 ± 1,2	1,9 ± 1,3	5,2 ± 1,9	
	3,3	4,0 ± 1,6	6,3 ± 1,5	10 ± 2	5 ± 2	5,7 ± 1,2	4 ± 3	1,0 ± 0,4	3,4 ± 1,3	2,7 ± 0,6	5,2 ± 1,9	
	4,4	4,6 ± 1,5	7 ± 2	11 ± 3	6,2 ± 1,8	5,7 ± 1,2	2,8 ± 1,5	0,7 ± 0,5	1,9 ± 1,5	2,6 ± 0,7	5,2 ± 1,9	
	5,5	4,9 ± 1,6	7 ± 3	11 ± 5	5,7 ± 1,2	5,3 ± 1,1	3 ± 2	0,4 ± 0,6	2,0 ± 0,6	2,3 ± 0,9	4,0 ± 1,6	

Table 2, top rows: measured relative intensity variations for the 10 events by assuming different projected altitude intervals and the same radial extensions for the circular crown areas and by using COR1 (top) and COR2 (bottom) data. Bottom rows: measured relative intensity variations for the 10 events by assuming different radial extensions for the circular crown areas and by using COR1 (top) and COR2 (bottom) data.

7. Algorithm optimization

For the optimization of the algorithm, two different tests have been performed, in particular: 1) the relative intensity variations measured for different altitude intervals covered by the circular crown areas, and 2) the relative intensity variations measured for different radial extensions of the circular crown areas. The first tests is aimed at identifying which region of the instrument field of view (e.g. inner part, outer part, or intermediate part) is more sensible to the CME transit; the second test is aimed at identifying the radial extension of regions in the instrument field of view to consider to maximize the intensity variation during the transit of the CME. The different circular crown areas are shown in Figure 5. The COR1 and COR2 data have been analysed to mimic the METIS observations that will be acquired both at 0.28 and 0.72 AU during the Solar Orbiter mission.

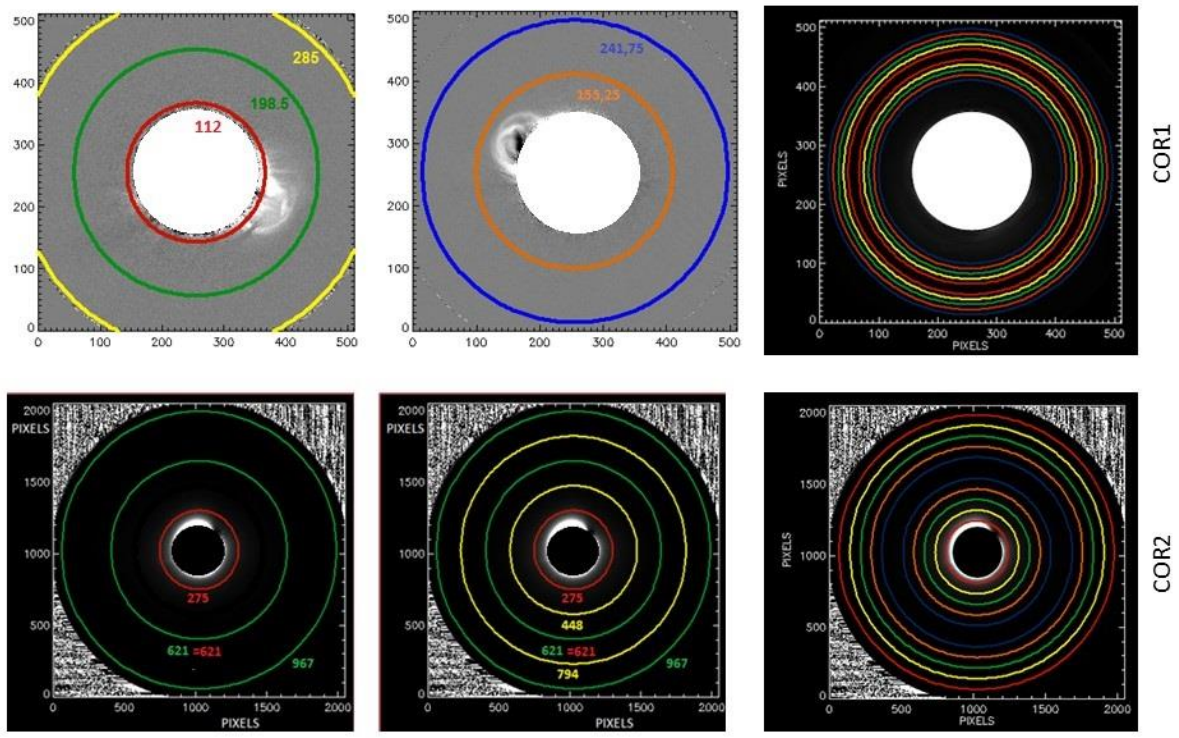

Figure 5: examples of different circular crown areas considered for the first test (left and middle columns) and the second test (right column) and based on the COR1 (top) and COR2 (bottom) data.

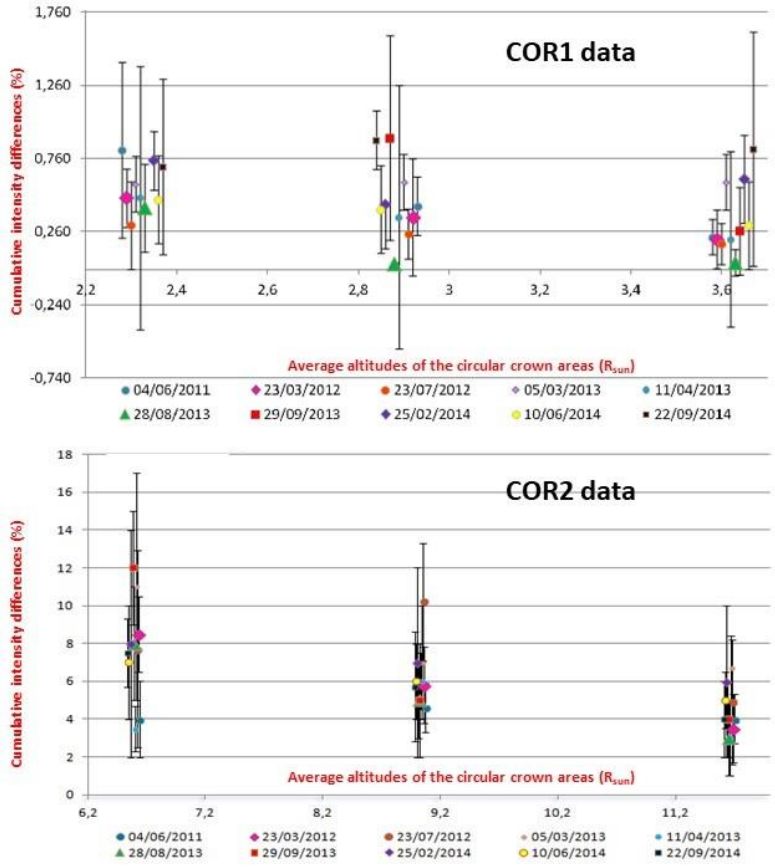

Figure 6: maxima relative intensity variations measured for the 10 events and by assuming 6 different values of the average altitude of circular crown areas, and by using COR1 (top) and COR2 (bottom) data.

7.1 Effects of different average altitudes

For the first test we considered 6 different locations for the average projected altitudes of the circular crown areas in the instrument field of views: 3 values for the COR1 data (2.32, 2.97 and 3.62 R_{sun}), and 3 values for the COR2 data (6.6, 9.0 and 11.6 R_{sun}). The radial extensions of different circular crown areas have been fixed to the same value of 86 pixels for COR1 data and 346 pixels for COR2 data. The resulting intensity variations measured for the 10 selected events are given in the top rows of Table 2 and are also shown in the plots of Figure 6. Results show that the sensitivity of the algorithm to different CMEs increases considering the circular crown areas that are located closer to the inner edge of the images.

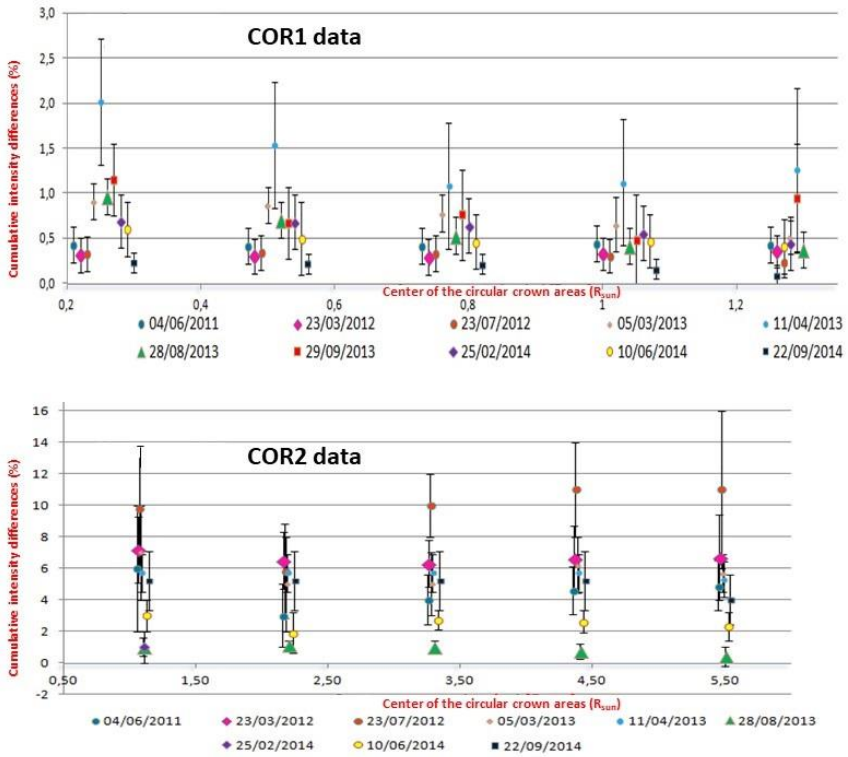

Figure 7: maxima relative intensity variations measured for the 10 events and by assuming 10 different values of the radial extensions of circular crown areas, and by using COR1 (top) and COR2 (bottom) data.

7.2 Effects of different radial extensions

For the second test we considered 10 different radial extensions of the circular crown areas in the instrument field of views: 5 values for the COR1 data, and 5 values for the COR2 data (see also the right column of Figure 5). The resulting intensity variations measured for the 10 selected events are given in the bottom rows of Table 2 and are also shown in the plots of Figure 7. Results show that the sensitivity of the algorithm to different CMEs is highly variable for different events, but more in general it decreases considering larger extensions of the circular crown areas.

8. Summary and conclusions

In this work we focused on the optimization of the on-board algorithm of the METIS coronagraph for the automatic identification of solar Coronal Mass Ejections (CMEs). For this purpose, we selected 10 CMEs from the SEEDS catalogue and downloaded 900 fits files acquired from the COR1 and COR2 coronagraphs to take into account the variations in the projected heliocentric distances that will be covered by METIS along the Solar Orbiter mission. These images correspond to 300 polarized triplets, acquired with 3 different

orientations of the linear polarizer. On the other hand, because METIS acquires quadruplets of polarized images with 4 different orientations of the linear polarizer, in this work from each triplet we obtained the 3 components of the Stokes vector (I, Q, U) and then built 1200 polarized quadruplets to simulate the METIS data.

We have then created a routine that (as it is done by the on-board algorithm) extracts the intensities in circular crown areas averaged over 8 angular sectors and by taking into account the different orientations of the polarizer. In order to optimize the algorithm, we measured the relative intensity variations for the selected events by assuming 1) different average altitudes covered by the circular crown areas, and 2) different radial extensions of the circular crown areas.

Results show that the algorithm is always able to determine the occurrence of CMEs and the main latitude of CMEs at both 0.28 and 0.72 AU, and will be optimized (i.e. will measure the maximum temporal variation of running differences):

- by averaging the signal on the innermost circular crown areas, and
- by averaging the signal on circular crown areas with smaller radial extensions.

Taking into account these constraints on the one hand, and also taking into account the S/N ratio on the other hand (hence uncertainties in the estimate of relative running differences), will guarantee the optimal operation of the on-board algorithm for the automated detection of CMEs.

References

Antonucci, E.; Romoli, M.; Andretta, V.; Fineschi, S.; Heinzel, P.; Moses, J. D.; Naletto, G.; Nicolini, G.; Spadaro, D.; Teriaca, L.; Berlicki, A.; Capobianco, G.; Crescenzio, G.; Da Deppo, V.; Focardi, M.; et al.; "Metis: the Solar Orbiter visible light and ultraviolet coronal imager", Astronomy & Astrophysics, Volume 642, id.A10, 41 pp. (2020).

Bemporad, A.; "The orbit of Solar Orbiter: characterization and implications for the METIS coronagraph (part 1)", OATO Tech. Rep. n. 125, https://openaccess.inaf.it/handle/20.500.12386/632 (2009)

Bemporad, A.; Andretta, V.; Pancrazzi, M.; Focardi, M.; Straus, T.; Sasso, C.; Spadaro, D.; Uslenghi, M.; Antonucci, E.; Fineschi, S.; Abbo, L.; Nicolini, G.; Landini, F.; Romoli, M.; Naletto, G.; Nicolosi, P.; "On-board CME detection algorithm for the Solar Orbiter-METIS coronagraph", Proceedings of the SPIE, Volume 9152, id. 91520K 11 pp. (2014).

Fineschi, S.; Naletto, G.; Romoli, M.; Da Deppo, V.; Antonucci, E.; Moses, D.; Malvezzi, A. M.; Nicolini, G.; Spadaro, D.; Teriaca, L.; Andretta, V.; Capobianco, G.; Crescenzio, G.; Focardi, M.; et al.; "Optical design of the multi-wavelength imaging coronagraph Metis for the solar orbiter mission", Experimental Astronomy, Volume 49, Issue 3, p.239-263 (2020).

Olmedo, O.; Zhang, J.; Wechsler, H.; Poland, A.; Borne, K.; "Automatic Detection and Tracking of Coronal Mass Ejections in Coronagraph Time Series", Solar Physics, Volume 248, Issue 2, pp.485-499 (2008)

Pancrazzi, M.; Focardi, M.; Nicolini, G.; Andretta, V.; Uslenghi, M.; Magli, E.; Ricci, M.; Bemporad, A.; Spadaro, D.; Landini, F.; Romoli, M.; Antonucci, E.; Fineschi, S.; Naletto, G.; Nicolosi, P.; Teriaca, L.; "Hardware and software architecture on board solar orbiter/METIS: an update", Proceedings of the SPIE, Volume 9144, id. 91443F 13 pp. (2014).